# Zinc Metallo-$\beta$-Lactamase from *Bacteroides fragilis*: A Quantum Chemical Study on Model Systems of the Active Site

**Natalia Díaz, Dimas Suárez,† and Kenneth M. Merz, Jr.***

*Contribution from the Departamento de Química Física y Analítica, Universidad de Oviedo, Julián Clavería 33006, Oviedo. Spain, and 152 Davey Laboratory, Department of Chemistry, The Pennsylvania State University, University Park, Pennsylvania 16802-6300*

*Received December 21, 1999*

**Abstract:** Quantum chemical optimizations of the small model systems $([Zn(NH_3)_3(H_2O)]^{2+}$, $[Zn(NH_3)_3(OH)]^{+}$, $[Zn(NH_3)(SH)\ (HCOO)(OH)]^{-1}(H_2O)$ and $[Zn(NH_3)(SH)(HCOO)(H_2O)]\ (H_2O))$ were performed at different levels of quantum mechanical theory (HF/6-31G*, B3LYP/6-31G*, and MP2/6-31G*) to characterize the Zn−ligand bonds for the Zn1 and Zn2 binding sites of metallo-$\beta$-lactamases. The nature of the zinc coordination environment was further studied by considering larger mononuclear complexes at the B3LYP/6-31G*//HF/6-31G* level of theory ($[Zn(Me\text{-}Im)_3(H_2O)]^{2+}$, $[Zn(Me\text{-}Im)(SCH_3)(CH_3COO)(H_2O)](H_2O)$, etc.). The structure and properties of a series of binuclear model compounds showing an hydroxy-mediated Zn1···Zn2 interaction were also analyzed at the same level of theory. One of the binuclear models with a global charge of +2, reproduces the main structural features of the *Bacteroides fragilis* active site as determined by X-ray crystallography. The proposed $\beta$-lactamase model has a monoprotonated state characterized by a strong H-bond interaction between a zinc-shared water molecule and a Zn2-bound Asp carboxylic group. The theoretical results are discussed in the context of experimental kinetic and structural data on the *B. fragilis* active site, resulting in insights into the nature of the zinc−ligand interactions, the location of the mechanistically relevant water molecules, and the actual protonation state of the active site. By combining the present results with previous theoretical and experimental work, mechanistic details for the mode of action of zinc $\beta$-lactamases are discussed.

## Introduction

$\beta$-lactam antibiotics account for 50% of the world's total antibiotic market.[1] The various families of $\beta$-lactam antibiotics differ in their spectrum of antibacterial activity and in their susceptibility to $\beta$-lactamase enzymes. $\beta$-lactamases, which constitute the most common and growing form of antibacterial resistance,[2,3] catalyze the hydrolysis of $\beta$-lactams to give ring-opened $\beta$-amino acids which are no longer effective as inhibitors against their targets: bacterial membrane-bound transpeptidases enzymes.

The mechanistic division of $\beta$-lactamases is into serine proteases (classes A, C, and D; according to their amino acid sequence homology) and zinc enzymes (class B).[3] For the serine proteases, the catalytic mechanism involves the formation of an acyl enzyme intermediate generated by the nucleophilic attack on the $\beta$-lactam of the hydroxyl group of the essential serine residue.[3] Fortunately, through the screening of natural chemical resources (i.e., plants) as well as through molecular studies on serine $\beta$-lactamases effective inhibitors have been discovered (e.g., cefoxitin, clavulanic acid, penicillanic acid sulfones, etc.).[4] These and other mechanism-based inhibitors selectively prevent substrate binding between $\beta$-lactamases and $\beta$-lactams while not interfering with cellular metabolism. On the other hand, the metallo-$\beta$-lactamases[5] (class B) require Zn(II) ions for their ability to efficiently hydrolyze nearly all $\beta$-lactams including the versatile broad-spectrum antibacterial carbapenem derivatives (see Scheme 1).

**Scheme 1**

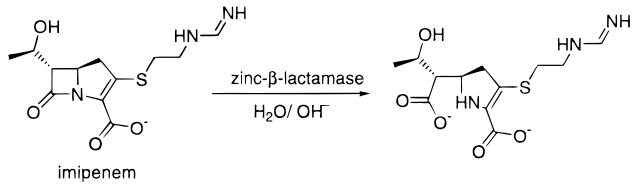


The first metallo-$\beta$-lactamase to be identified was found in the relatively innocuous bacteria *Bacillus cereus* in the 1960s. Since this time most mechanistic and structural information of Zn-$\beta$-lactamases has been derived from the *B. cereus* enzyme.[6−10] This enzyme is remarkably adaptable and is able to function with either one or two zinc ions, which are liganded by active-

† On leave from Departamento de Química Física y Analítica, Universidad de Oviedo, Spain.

(1) *The Chemistry of β-Lactams*. Page, M. I., Ed.; Blackie Academic&Professional: London, 1992.

(2) Page, M. I. *Chem. Commun.* **1998**, 1609−1617.

(3) Waley, S. G. $\beta$-lactamase: mechanism of action. In ref 1, pp 199−228.

(4) Pratt, R. F. $\beta$-lactamase: Inhibition. In ref 1, pp 229−265.

(5) Wang, Z.; Fast, W.; Valentine, A. M.; Benkovic, S. J. *Curr. Opin. Chem. Biol.* **1999**, *3*, 614−622.

(6) Paul-Soto, R.; Zeppezauer, M.; Adolph, H. W.; Galleni, M.; Frère, J. M.; Carfi, A.; Dideberg, O.; Wouters, J.; Hemmingsen, L.; Bauer, R. *Biochemistry* **1999**, *38*, 16500−16506.

(7) Paul-Soto, R.; Bauer, R.; Frère, J. M.; Galleni, M.; Meyer-Klaucke, W.; Nolting, H.; Rossolini, G. M.; de Seny, D.; Hernández-Valladares, M.; Zeppezauer, M.; Adolph, H. W. *J. Biol. Chem.* **1999**, *274*, 13242−13249.

(8) Fabiane, S. M.; Sohi, M. K.; Wan, T.; Payne, D. J.; Bateson, J. H.; Mitchell, T.; Sutton, B. J. *Biochemistry* **1998**, *37*, 12404−12411.

(9) Carfi, A.; Duée, E.; Galleni, M.; Frère, J. M.; Dideberg, O. *Acta Crystallogr. D* **1998**, *54*, 313−323.

(10) Bounaga, S.; Laws, A. P.; Galleni, M.; Page, M. I. *Biochem. J.* **1998**, *331*, 703−711.

10.1021/ja994462s CCC: $19.00 
Published on Web 04/18/2000

**Scheme 2**

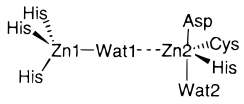


**Scheme 3**

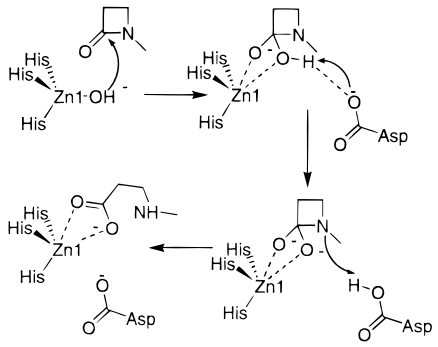


site residues that are generally conserved in all known metallo-$\beta$-lactamase sequences. The first zinc ion, Zn1 in Scheme 2, is coordinated by three histidine residues and a water molecule in a tetrahedral arrangement.[6,8,9] The second zinc ion, Zn2, which may be present or not, depending on the enzyme:$Zn^{2+}$ molar ratio, is coordinated by the carboxylate group of an aspartate, the methylthiolate group of a cysteine, the imidazole ring of a histidine, the Zn1-bound Wat1 molecule, and a second water molecule, Wat2. The resulting coordination environment for Zn2 is a distorted trigonal bipyramidal arrangement.[6,8,9] Interestingly, Zn1 is tightly bound by the histidines and Wat1, while Zn2 is located at a large distance from Zn1 (3.9−4.4 Å).[6,8] Moreover, in one of the reported di-zinc structures,[8] the Zn2 ion shows a very "loose" arrangement of the ligands, that is, the Zn2-ligand bond distances lie in the range 2.5−3.0 Å except for the Zn2•••$S_\gamma$(Cys) interatomic distance which is close to 2.0 Å. This is in agreement with the low affinity of the enzyme for the second Zn ion (~24 mM) with respect to that of Zn1 (~1 $\mu$M).[10]

One of the proposed mechanisms[8,10] for the action of the *B. cereus* $\beta$-lactamase, assumes that the Zn1-bound water, present in its unprotonated form at neutral pH, would attack the $\beta$-lactam carbonyl, forming an acyl enzyme intermediate. The interaction between the Zn1 cation and the negative charge developed on the $\beta$-lactam oxygen atom would stabilize the intermediate (see Scheme 3). Subsequently, the Asp residue, initially H-bonded to the Wat1 molecule and coordinated to the Zn2 position in the binuclear enzyme, would accept a proton from the hydroxyl moiety in the intermediate and, as the $\beta$-lactam C−N bond fission proceeds, protonate the leaving amino group. According to kinetic data, the rate-determining step would correspond to one of the two proton-transfer processes.[10] This mechanistic proposal implies the participation of a di-anionic species which could explain the second-order dependence of reactivity on the $H^+$ concentration at low pH. This mechanism has no significant role for the second zinc ion, which is portrayed as being more important for substrate binding. For the binuclear *B. cereus* enzyme, it has recently been reported that its catalytic efficiency is only marginally superior to that of the mononuclear form with some substrates and is even lower with other ones.[7]

In addition to the prototypical class B $\beta$-lactamase from *B. cereus*, there are now at least 20 bacterial sources of metallo-$\beta$-lactamases, including those from pathogenic strains of *Pseudomonas maltophilia*,[11,12] *Aeromonas sobria*,[13] and, *Bacteroides fragilis*.[14−23] The Zn-$\beta$-lactamase from *B. fragilis*, which is a Gram-negative anaerobic bacteria associated with post-surgical hospital infections, exhibits the most efficient activity and the broadest spectrum for different $\beta$-lactam substrates.[5,14,16] Moreover, as a plasmid encoded enzyme, the *B. fragilis* Zn $\beta$-lactamase is able to spread to other pathogenic bacteria. At present there are no clinically useful inhibitors known against the broad-spectrum zinc-$\beta$-lactamases in contrast to those against the serine enzymes.[4] This clearly stresses the importance and urgency of increasing our understanding of the structure, dynamics, and catalytic mechanism of the zinc-$\beta$-lactamases, thereby, providing a rational basis for future drug design efforts.

X-ray crystallographic studies have revealed that the active site of the *B. fragilis* enzyme contains two Zn ions of comparable affinity (~1 $\mu$M), which are located close to one another (3.3−3.5 Å).[14−18] In this structure, the Zn1 ion is coordinated by the imidazole groups from three different histidine residues. In contrast with the *B. cereus* enzyme, the second zinc ion in the *B. fragilis* active site is tightly coordinated by the carboxylate, the thiolate, another imidazole group, and the second water molecule. In addition, two of the structural determinations[14,16] have observed the presence of a shared water/hydroxide molecule bridging Zn1 and Zn2. Therefore, the active site resembles a Zn binuclear complex in which a distorted tetrahedron (Zn1) and a trigonal bipyramid (Zn2) are connected through an intermediate ligand. This structural arrangement is in agreement with the increased affinity of the *B. fragilis* enzyme for the second Zn ion in its active site.

Recently, the catalytic mechanism of the metallo-$\beta$-lactamase from *B. fragilis* has been experimentally investigated using nitrocefin as substrate.[20−22] These studies revealed the existence of an acyl enzyme intermediate which presents a negatively charged nitrogen-leaving group and, most likely, the cleavage of the $\beta$-lactam ring.[21] On the basis of the various experimental results, a qualitative mechanism of the binuclear *B. fragilis* enzyme has been proposed[22] (see Scheme 4, residue numbering taken from ref 14) which is similar to those proposed for other binuclear zinc hydrolases.[24] The Zn1-hydroxide nucleophile directly attacks the $\beta$-lactam carbonyl group with the simultaneous fission of the C−N bond to give the negatively charged N atom species detected experimentally.[20] The formation of this unusual intermediate could be favored through strong electrostatic interactions with the Zn2 ion after the Wat2 molecule is displaced from the Zn2 coordination environment. The break-

(11) Ullah, J. H.; Walsh, T. R., Taylor, I. A.; Emery, D. C.; Verma, C. S.; Gamblin, S. J.; Spencer, J. *J. Mol. Biol*. **1998**, *284*, 125−136.
(12) McManus-Muñoz, S.; Crowder, M. W. *Biochemistry* **1999**, *38*, 1547−1553.
(13) Walsh, T. R.; Gamblin, S.; Emery, D. C.; MacGowan, A. P.; Bennetm, P. M. *J. Antimicrob. Chemother*. **1996**, *37*, 423−441.
(14) Concha, N. O.; Rasmussen, B. A.; Bush, K.; Herzberg, O. *Structure* **1996**, *4*, 623−635. PDB Entry: 1ZNB.
(15) Carfi, A.; Duée, E.; Paul-Soto, R.; Galleni, M.; Frère, J. M.; Dideberg, O. *Acta Crystallogr. D* **1998**, *54*, 47−57. PDB Entry: 1BMI.
(16) Fitzgerald, P. M. D.; Wu, J. K.; Toney, J. H. *Biochemistry* **1998**, *37*, 6791−6800. PDB Entry: 1A7T.
(17) Toney, J. H.; Fitzgerald, P. M. D.; Grover-Sharma, N.; Olson, S. H.; May, W. J.; Sundelof, J. G.; Vanderwall, D. E.; Cleary, K. A.; Grant, S. K.; Wu, J. K.; Kozarich, J. W.; Pompliano, D. L.; Hammond, G. G. *Chem. Biol*. **1998**, *5*, 195−196.
(18) Li, Z.; Rasmussen, B. A.; Herzberg, O. *Protein Sci*. **1999**, *8*, 249−252.
(19) Crowder, M. W.; Wang, Z.; Franklin, S. L.; Zovinka, E. P.; Benkovic, S. J. *Biochemistry* **1996**, *35*, 12126−12132.
(20) Wang, Z.; Benkovic, S. J. *J. Biol. Chem*. **1998**, *273*, 22402−22408.
(21) Wang, Z.; Fast, W.; Benkovic, S. J. *J. Am. Chem. Soc.* **1998**, *120*, 10778−10779.
(22) Wang, Z.; Fast, W.; Benkovic, S. J. *Biochemistry* **1999**, *38*, 10013−10023.
(23) Paul-Soto, R.; Hernández-Valladares, M.; Galleni, M.; Bauer, R.; Zeppezauer, M.; Frère, J. M.; Adolph, H. W. *FEBS Lett*. **1998**, *438*, 137−140.
(24) Lipscomb, W. N.; Sträter, N. *Chem Rev*. **1996**, *96*, 2375−2433.

**Scheme 4**

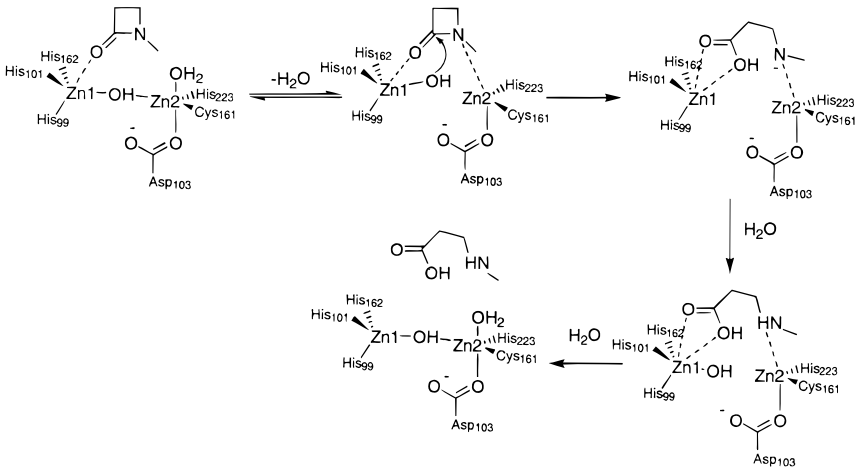

down of the intermediate constitutes the rate-determining step of the process.[21,22] It has been suggested that water molecules from bulk solvent could protonate the negatively charged N atom and, finally, loss of the acyl group from Zn1 regenerates the active site for the next turnover. Although the dizinc form of the *B. fragilis* β-lactamase is normally considered as the biologically active form, it has been recently reported that the *B. fragilis* Zn-β-lactamase is also active with a mononuclear zinc site, which suggests that there are distinct mechanisms for the mono- and binuclear species.[23]

Computationally tractable model systems offer a valuable approach toward understanding biological catalysis.[25] Theoretical work has been devoted to the investigation of the neutral and alkaline hydrolysis of β-lactams since the knowledge of the molecular mechanism of these processes could be of great importance in the development of new antibacterial drugs and β-lactamase inhibitors.[26−28] The characterization of water-assisted and nonassisted reaction pathways between 2-azetidinones and the hydroxide anion[26,27] are of interest for understanding the mode of action of class B β-lactamases. It has been found that this model reaction proceeds through the formation of a negatively charged tetrahedral complex, the corresponding energy barrier being determined by the desolvation of the hydroxide anion. Most interestingly, the subsequent ring opening of the acyl intermediate and proton transfer to the leaving amino group can take place asynchronously, that is, involving the participation of an unstable ring-opened species with a negatively charged N atom similar to that proposed in the *B. fragilis* mechanism. Nonetheless, other mechanistic pathways are similar in energy and, therefore, the actual mechanism for the ring-opening of the acyl intermediate could be greatly influenced by β-lactam substituents, solution, protein environment, etc.[27]

As one of the first applications of computational methods to specifically investigate zinc β-lactamases the relationship between the active-site geometry of the *B. fragilis* enzyme and the electronic spectra of the cobalt-substituted enzyme has been addressed.[29] The spectroscopic calculations have predicted that the observed visible and UV transitions result from the Zn1 and Zn2 cobalt-substituted positions, respectively while some differences and similarities between the *B. cereus* and *B. fragilis* spectra have been rationalized. However, the structural calculations reported[26] were limited to what was necessary to analyze the electronic spectra and the native *B. fragilis* crystal structure[14] used to build the model compounds.

From previous theoretical and experimental work on the structure and function of Zn β-lactamases, it is clear that a computational examination of model systems representing the coordination of the $Zn^{2+}$ ions in the active site of the *B. fragilis* and *B. cereus* enzymes may improve our understanding of the zinc-β-lactamases. A large set of model compounds, which include both mononuclear and binuclear zinc complexes, are analyzed in this work by means of quantum chemical methods capable of providing a well-balanced description of the ligand binding ability of the Zn ions. The examination of the *B. fragilis* model systems provide insights into the nature of the contacts between the zinc ligands, the location of the mechanistically relevant water molecules, the actual protonation state of the active site, etc. Similarly, further insights into the differences in the structure and function between the β-lactamases from *B. cereus* and *B. fragilis* have been garnered. Finally, the mechanistic implications of the present results for the catalytic action of the zinc-β-lactamases will be discussed.

## Methods

Ab initio calculations were carried out with Gaussian 98.[30] All of the optimizations were done in the gas phase with no constraints. The initial geometries for the mononuclear and binuclear complexes were built by molecular modeling from the X-ray coordinates of *B. fragilis* (PDB ID code: 1ZNB).[14]

For the first set of mononuclear complexes studied: $[Zn(NH_3)_3(H_2O)]^{2+}$, $[Zn(NH_3)_3(OH)]^{+}$, $[Zn(NH_3)(SH)(HCOO)(OH)]^{-1}(H_2O)$, and $[Zn(NH_3)(SH)(HCOO)(H_2O)]$, geometries were optimized at the HF/6-31G*, B3LYP/6-31G*, and MP2/6-31G* levels of theory[31−33] and further characterized by analytic computation of harmonic frequencies

(25) Tantillo, D. J.; Chen, J.; Houk, K. N. *Curr. Opin. Chem. Biol.* **1998**, *2*, 743−750.

(26) Pitarch, J.; Ruiz-López, M. F.; Pascual-Ahuir, J. L.; Silla, E.; Tuñón, I. *J. Phys. Chem* **1997**, *101*, 3581−3588.

(27) Pitarch, J.; Ruiz-López, M. F.; Silla, E.; Pascual-Ahuir, J. L.; Tuñón, I. *J. Am. Chem. Soc.* **1998**, *120*, 2146−2155.

(28) Frau, J.; Donoso, J.; Muñoz, F.; Vilanova, B.; García-Blanco, F. *Helv. Chim. Acta*. **1997**, *80*, 739−747.

(29) Hilson, H. S. R.; Krauss, M. *J. Am. Chem. Soc.* **1999**, *121*, 6984−6989.

(30) Frisch, M. J.; Trucks, G. W.; Schlegel, H. B.; Scuseria, G. E.; Robb, M. A.; Cheeseman, J. R.; Zakrzewski, V. G.; Montgomery, J. A.; Stratmann, R. E., Jr.; Burant, J. C.; Dapprich, S.; Millam, J. M.; Daniels, A. D.; Kudin, K. N.; Strain, M. C.; Farkas, O.; Tomasi, J.; Barone, V.; Cossi, M.; Cammi, R.; Mennucci, B.; Pomelli, C.; Adamo, C.; Clifford, S.; Ochterski, J.; Petersson, G. A.; Ayala, P. Y.; Cui, Q.; Morokuma, K.; Malick, D. K.; Rabuck, A. D.; Raghavachari, K.; Foresman, J. B.; Cioslowski, J.; Ortiz, J. V.; Stefanov, B. B.; Liu, G.; Liashenko, A.; Piskorz, P.; Komaromi, I.; Gomperts, R.; Martin, R. L.; Fox, D. J.; Keith, T.; Al-Laham, M. A.; Peng, C. Y.; Nanayakkara, A.; Gonzalez, C.; Challacombe, M.; Gill, P. M. W.; Johnson, B.; Chen, W.; Wong, M. W.; Andres, J. L.; Gonzalez, C.; Head-Gordon, M.; Replogle, E. S.; Pople, J. A. *Gaussian 98*, revision A.6; Gaussian, Inc.: Pittsburgh, PA, 1998.

**Table 1.** Total Energies (au), Relative Energies in Parentheses (kcal/mol), and Gas-Phase Proton Affinities PA (kcal/mol) for the **1/1$_H$** and **2/2$_H$** Complexes

| structures | | HF/6-31G* | ZPVE[a] | B3LYP/ 6-31G*// HF/6-31G* | B3LYP/ 6-31G* | MP2/ 6-31G* | CCSD(T)/ 6-31G*[b] | MP2/ 6-311+ G(3df,2p)[b,c] | PA[d] |
|---|---|---|---|---|---|---|---|---|---|
| $[Zn(NH_3)_3(\mathbf{OH})]^+$ | **1** | −2021.426206 | 0.137848 | −2024.495007 | −2024.498383 | −2022.383029 | −2022.423902 | −2022.788856 | |
| | | (0.0) | (0.0) | (0.0) | (0.0) | (0.0) | (0.0) | (0.0) | − |
| $[Zn(NH_3)_3(\mathbf{H_2O})]^{2+}$ | $\mathbf{1_H}$ | −2021.691257 | 0.151347 | −2024.749065 | −2024.752351 | −2022.753394 | −2022.681392 | −2023.036681 | |
| | | (−166.3) | (8.5) | (−159.4) | (−159.4) | (−159.9) | (−161.6) | (−155.5) | **150.4** |
| $[Zn(NH_3)(SH)(HCOO)(\mathbf{OH})]^{-1}(H_2O)$ | **2** | −2571.597282 | 0.116488 | −2576.049008 | −2576.056920 | −2573.007611 | −2573.066173 | −2573.699253 | |
| | | (0.0) | (0.0) | (0.0) | (0.0) | (0.0) | (0.0) | (0.0) | − |
| $[Zn(NH_3)(SH)(HCOO)(\mathbf{H_2O})](H_2O)$ | $\mathbf{2_H}$ | −2572.140193 | 0.131189 | −2576.590770 | −2576.598356 | −2573.545266 | −2573.607278 | −2574.229241 | |
| | | (−340.6) | (9.2) | (−340.0) | (−339.8) | (−337.4) | (−339.5) | (−332.6) | **326.9** |

[a] From HF/6-31G* analytical frequencies. [b] Single-point calculations on the MP2/6-31G* geometries. [c] 6-31G* basis set for Zn. [d] Using an additive combination of electronic energies (CCSD(T)/6-31G* + MP2/6-311+G(3df,2p) -MP2/6-31G*) and HF/6-31G* thermal corrections.

at the HF/6-31G* level. Thermodynamic data (298 K, 1 bar) were computed using the HF/6-31G* frequencies within the ideal gas, rigid rotor, and harmonic oscillator approximations.[34] To estimate the effect of larger basis sets and more elaborate *N*-electron treatments on the relative energies,[35] CCSD(T)/6-31G* and MP2/6-311+G(3df,2p)[6-31G* for Zn] single-point calculations on the MP2/6-31G* geometries were also performed.

The second set of mononuclear models comprises four different structures $[Zn(Me\text{-}Im)_3(H_2O)]^{2+}$, $[Zn(Me\text{-}Im)_3(OH)]^+$, $[Zn(Me\text{-}Im)(SCH_3)(CH_3COO)(H_2O)](H_2O)$, and $[Zn(Me\text{-}Im)(SCH_3)(CH_3COO)(OH)]^{-1}(H_2O)$ all of which were optimized at the HF/6-31G* level of theory followed by analytic computation of the harmonic frequencies. Electronic energies were then recalculated at the B3LYP/6-31G* level using the HF/6-31G* geometries.

The binuclear models of the zinc-$\beta$-lactamases active sites reported in this work were fully optimized at the HF/6-31G* level and the electronic energies recalculated at the B3LYP/6-31G* level. The large size of the binuclear systems (67−68 atoms, around 600 basis functions) prevented us from carrying out HF/6-31G* frequency calculations. For the binuclear structures which could be located on the HF/3-21G* potential energy surface (PES), the corresponding analytical Hessians were also calculated at the HF/3-21G* level.

Using Bader's theory of atoms in molecules,[36] the nature of the Zn−ligand bonds was further analyzed by calculating the corresponding bond critical point (BCP) properties in the charge density $\rho(\mathbf{r_c})$. The values of $\rho(\mathbf{r_c})$, $\nabla^2\rho(\mathbf{r_c})$ and of the local energy density[37] $H(\mathbf{r_c})$ at the BCPs enable one to characterize the interatomic interactions. The most important BCP properties of all of the systems studied in this work are reported as Supporting Information. The BCP analysis employed a recent version of the EXTREME program, a part of the AIMPAC suite of programs.[38]

The electrostatically derived atomic charges (EPS) were also computed for all of the structures according to the Merz−Kollman−Singh scheme.[39]

## Results

The protonation state of the *B. fragilis* active site is still a matter of conjecture; thus, to address this issue we optimized several conjugate acid−base pairs of model compounds representing the Zn1 and Zn2 coordination environment in Zn $\beta$-lactamases. We first present the results on the mononuclear complexes $[Zn(NH_3)_3(OH)]^+$(**1**) and $[Zn(NH_3)(SH)(HCOO)(OH)]^{-1}(H_2O)$ (**2**), including their corresponding acid forms $\mathbf{1_H}$ and $\mathbf{2_H}$. Subsequently, we carried out HF/6-31G* optimizations of mononuclear Zn compounds liganded by methyl-imidazole, acetate, and methylthiolate, thereby simulating the side chains of the corresponding histidine, aspartate, and cysteine residues bound to the Zn ions in the $\beta$-lactamase active site. These mononuclear complexes constitute an appropriate set of reference structures that can be useful to subsequently analyze the inherent features of the binuclear model systems.

**Mononuclear Complexes $\mathbf{1_H}$/1 and $\mathbf{2_H}$/2: Influence of the Level of Theory.** Table 1 presents the relative energies, while Figure 1 displays the corresponding minimized structures. The equilibrium geometries, charge distribution, and protonation energies of these compounds were examined at different levels of theory in order to calibrate the methodology to be used in the determination of the energetics and structures of the model systems discussed below.

Supporting Information includes tables of the BCP properties for the $\mathbf{1_H}$/**1** and $\mathbf{2_H}$/**2** complexes and for the rest of structures studied in this work. The analysis of the charge density is a useful complement to geometrical observations. We found that all of the specific zinc−ligand interactions in these complexes may be characterized as closed-shell interactions since the charge density at the corresponding BCP $\rho(\mathbf{r_c})$ is relatively low in value, the Laplacian $\nabla^2\rho(\mathbf{r_c})$ is positive, and the ellipticity at BCP $\epsilon$ is close to zero. However, we note that the zinc−ligand bonds have a certain character of intermediate interactions, that is, involving a partial covalent character, since the magnitude of the $\rho(\mathbf{r_c})$ values (0.06−0.08 au) represents a significant accumulation of charge in the interatomic region.[36] The zinc−ligand BCP properties depend notably on the *hard*−*soft* character of the ligand→$Zn^{2+}$ charge transfer, revealing more clearly how the zinc coordination environment is affected by ligand-exchange and protonation processes.

Zinc ammonia−water complexes such as $\mathbf{1_H}$/**1** have been previously studied using different levels of theory as simple models of the carbonic anhydrase active site.[40] We see in Figure 1 that the Zn−N and Zn−O bond distances in the tetrahedral complexes $\mathbf{1_H}$/**1** are lengthened and shortened by 0.04 Å (∼2%) and 0.20 Å (∼10%), respectively, upon deprotonation of **1**. In terms of the BCP properties the Zn−N $\rho(\mathbf{r_c})$ values decrease

(31) Hehre, W.; Radom, L.; Pople, J. A.; Schleyer, P. v. R. *Ab Initio Molecular Orbital Theory*; John Wiley & Sons Inc.: New York, 1986.

(32) Becke, A. D. Exchange-Correlation Approximation in Density-Functional Theory. In *Modern Electronic Structure Theory Part II*; Yarkony, D. R., Ed.; World Scientific: Singapore, 1995.

(33) The recently derived 6-31G* basis set for Zn was used in the geometry optimizations. See Rasolov, V. A.; Pople, J. A.; Patner, M. A.; Windus, T. L. *J. Chem. Phys.* **1998**, *109*, 1223−1230.

(34) McQuarrie, D. A. *Statistical Mechanics*; Harper & Row: New York, 1976.

(35) Raghavachari, K.; Curtiss, L. A. *Evaluation of Bond Energies to Chemical Accuracy by Quantum Chemical Techniques.* In *Modern Electronic Structure Theory Part II*; Yarkony, D. R., Ed.; World Scientific: Singapore, 1995.

(36) Bader, R. F. W. *Atoms in Molecules. A Quantum Theory*; Clarendon Press: Oxford, 1990.

(37) Grimme, S. *J. Am. Chem. Soc.* **1996**, *118*, 1529−1534.

(38) Biegler-König, F. W.; Bader, R. F. W.; Wang, T. H. *J. Comput. Chem.* **1982**, *3*, 317−328.

(39) Besler, B. H.; Merz, K. M., Jr..; Kollman, P. A. *J. Comput. Chem.* **1990**, *11*, 431−439.

(40) (a) Zheng, Y. J.; Merz, K. M., Jr. *J. Am. Chem. Soc.* **1992**, *114*, 10498−10507. (b) Sakurai, M.; Furuki, T.; Inoue, Y. *J. Phys. Chem.* **1995**, *99*, 17789−17794.

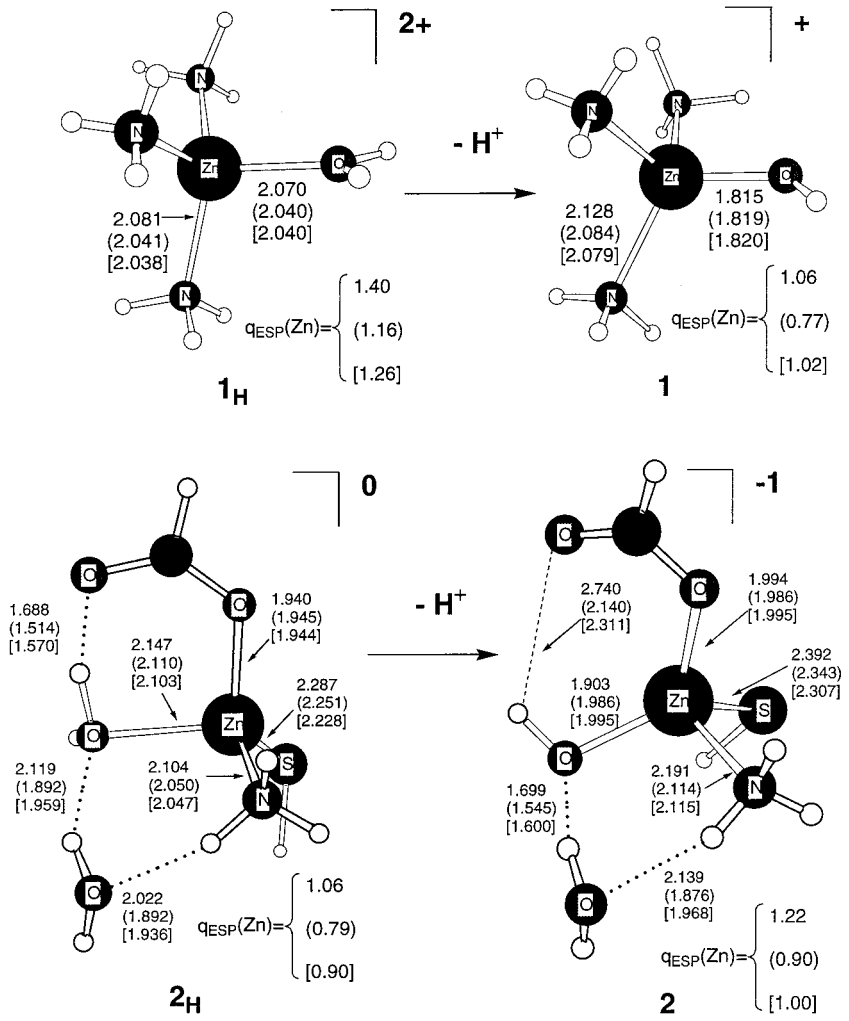


**Figure 1.** Optimized structures of the small mononuclear complexes $\mathbf{1_H/1}$ and $\mathbf{2_H/2}$. HF/6-31G*, (B3LYP/6-31G*), and [MP2/6-31G*] distances in Å. ESP charges for Zn are also indicated at the different levels of theory.

by 0.01 au (∼10%) upon deprotonation, while the Zn−O $\rho(\mathbf{r_c})$ increases from 0.06 to 0.12 au (∼50%). The resultant hydroxide moiety reinforces the charge transfer to the $Zn^{2+}$ cation by around 0.3 e. The hydroxide → Zn charge transfer, as well as the fact that the acid form bears a positive charge of +2, determines a relatively low value for the gas-phase PA of $\mathbf{1_H/1}$ (150.4 kcal/mol at the best level of theory).

The mononuclear structures $\mathbf{2_H/2}$ constitute preliminary model systems representing the coordination environment of the Zn2 ions in β-lactamases. In these complexes, the $Zn^{2+}$ ion binds four different ligands (hydroxide/water, ammonia, formate anion, and sulfide anion) that globally determine a much *harder* cavity around the $Zn^{2+}$ than that in the case of the positively charged $\mathbf{1_H/1}$ complexes. Examination of the data in Table 1 and Figure 1 reveals several interesting trends in the binding of the $\mathbf{2_H/2}$ zinc-complexes. The zinc ion has a coordination number of four in both structures in contrast with the trigonal-bipyramidal coordination observed experimentally for the Zn2 ion in the *B. fragilis* active site.[14] For the acid form $\mathbf{2_H}$, the configuration of the Zn site is close to a trigonal-pyramid (the O(Wat)-Zn−O(HCOO) and O(Wat)−Zn−N($NH_3$) angles are around 96−100°), but the second water molecule is preferentially located in the outer shell, hydrating the Zn-bound water and ammonia ligands. The carboxylate group and the metal-bound water molecule in $\mathbf{2_H}$ establish a strong H bond.[41] The geometry and BCP properties of this O−H···O contact show the relatively strong nature of this interaction which in turn is notably strengthened when electron correlation is considered: the O−H···O distance and $\rho(\mathbf{r_c})$ vary from 1.688 Å and 0.046 au at HF/6-31G* to 1.514 Å and 0.073 au, respectively, at the B3LYP/6-31G* level of theory. For comparative purposes, we characterized a typical H bond in a $CH_3COOH\cdots OH_2$ complex. This H bond has a distance of 1.897 Å and a $\rho(\mathbf{r_c})$ value of 0.028 au at the HF/6-31G* level (1.747 Å and 0.044 au at B3LYP/6-31G*). These structural and electronic data suggest that, in effect, the O−H···O contact in $\mathbf{2_H}$ is clearly strong and should have an increased covalency over the model complex.

Interestingly, a rearrangement around the $Zn^{2+}$ ion takes place when $\mathbf{2_H}$ loses a proton since the resultant basic form **2** shows a nearly tetrahedral ligand disposition which minimizes the charge repulsions among the formate, hydroxide, and sulfide groups and substantially weakens the intramolecular O−H···O contact (see Figure 1). The presence of a net negative charge on **2** "destabilizes" the ligand shell around the Zn ion, given that upon deprotonation the Zn−N, Zn−S, and Z−O(HCOO) distances all elongate by 0.05−0.2 Å, the corresponding $\rho(\mathbf{r_c})$ values are diminished by around 10%, and the positive charge on the Zn atom increases by +0.2 e. Given that **2** has a net negative charge, it is not surprising that **2** has a very high value of PA (326.9 kcal/mol at the best theory level, see Table 1).

The main structural and energetic characteristics of the conjugate acid−base pairs of the small zinc complexes are

(41) Perrin, C. L.; Melson, J. B. *Annu. Rev. Phys. Chem.* **1997**, *48*, 511−544.

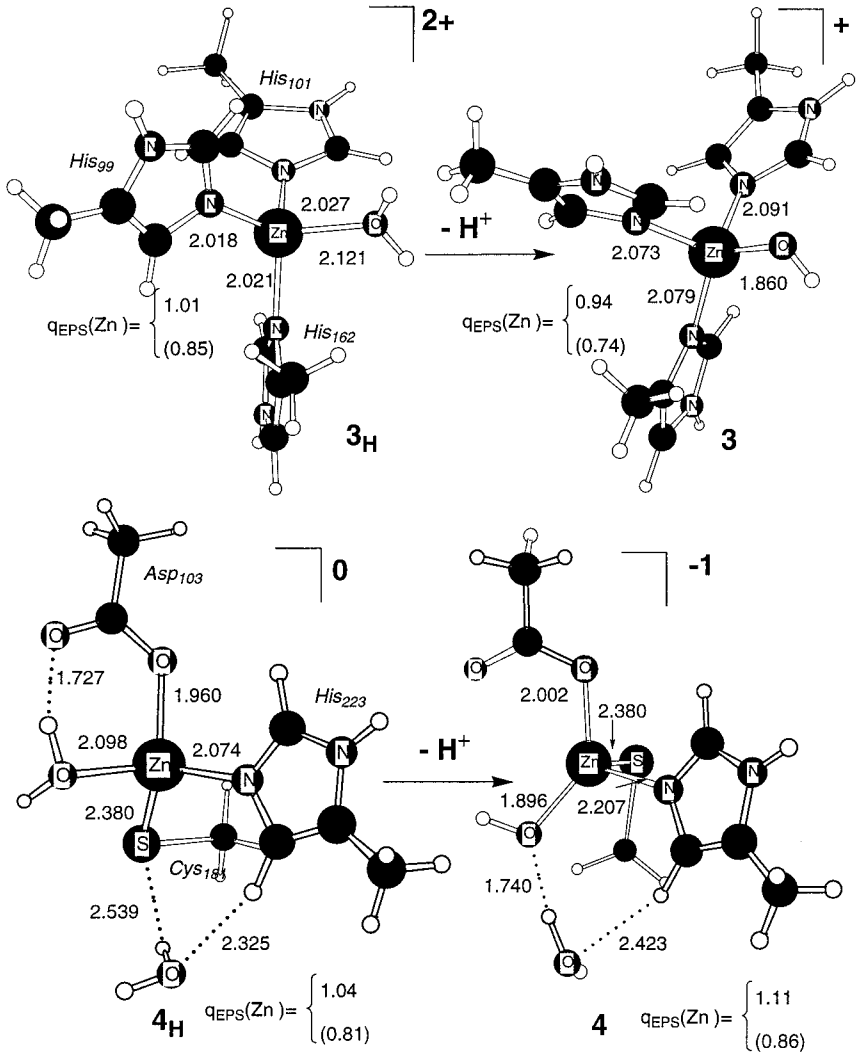


**Figure 2.** Optimized structures of the mononuclear complexes $\mathbf{3_H/3}$ and $\mathbf{4_H/4}$. HF/6-31G* and (B3LYP/6-31G*//HF/6-31G*) ESP charges for Zn are also indicated.

essentially the same at the HF level and at the correlated MP2 and B3LYP levels (see Figure 1 and Table 1). However some systematic differences can be observed when comparing the description of the Zn−ligand bonds at these levels of theory. The correlated methods give shorter Zn−N and Zn−S (∼ −0.02, −0.04 Å) and higher $\rho(\mathbf{r_c})$ values (∼ +0.01 au) and reinforce the O−H···O contacts with respect to the HF level of theory. For the Zn−O bonds, the HF/6-31G* and correlated levels provide similar descriptions. The B3LYP/6-31G* EPS charge for the Zn atom is systematically lower than the HF/6-31G* charges by 0.4−0.3 e, and the MP2/6-31G* charges are of intermediate value. These trends indicate that the HF/6-31G* level gives a greater emphasis to the contribution of electrostatics to the Zn−ligand bonds, whereas the MP2 and, especially, the B3LYP method seem to favor charge-transfer interactions for the Zn−N, Zn−S, and O−H···O bonds. Nevertheless, the calculated relative energies between the acid and basic forms are similar at all levels of theory, especially for $\mathbf{2_H/2}$ (see Table 1). Moreover, as is typical of organic bases,[42,43] single-point calculations on the MP2/6-31G* geometries indicate that the effects of a larger basis set, 6-311+G(3df,2p), and a more sophisticated correlation treatment (CCSD(T)) are relatively small in the calculation of PAs.

From the data in Figure 1 and Table 1, we conclude that the B3LYP/6-31G*//HF/6-31G* level can yield reasonable structures and energies for large systems. For example, when including the B3LYP/6-31G*//HF/6-31G* electronic energies, the calculated PAs for $\mathbf{1_H/1}$ and $\mathbf{2_H/2}$ are 152.6 and 332.3 kcal/mol, respectively. These values are only 5.8 and 5.4 kcal/mol above those obtained from composite CCSD(T) and MP2 electronic energies (see Table 1). Therefore, for the much larger zinc complexes analyzed in this work we used the B3LYP/6-31G*//HF/6-31G* level of theory.

**Mononuclear Complexes $\mathbf{3_H/3}$ and $\mathbf{4_H/4}$.** Previous work has shown that ammonia does not satisfactorily represent the Zn−N bond between the $Zn^{2+}$ ion and N atoms in imidazole rings.[40b,44] Apart from stereochemical considerations, the presence of the imidazole rings may have an important impact on the energetics of various processes. This is confirmed by our calculations on the $[Zn(Me\text{-}Im)_3(OH)]^+$ (**3**) and $[Zn(Me\text{-}Im)_3(H_2O)]^{2+}$ ($\mathbf{3_H}$) complexes (see Figure 2) since the PA value of the Zn-bound water increases dramatically from 152.6 to 184.6 kcal/mol when the ammonia ligands are replaced by 1-methyl-imidazole, the acid form $\mathbf{3_H}$ being preferentially stabilized (see Tables 1 and 2). In $\mathbf{3_H}$ the $Zn^{2+}$ ion is tightly bound by the N atoms from imidazole with distances close to 2.02 Å (around 2.08 Å in $\mathbf{1_H}$),

(42) Maksic, Z. B.; Kovacevic, B.; Kovacek, D. *J. Phys. Chem. A* **1997**, *101*, 7446−7453.
(43) Wasada, H.; Tsutsui, Y.; Yamabe, S. *J. Phys. Chem.* **1996**, *100*, 7367−7371.
(44) Lu, D.; Woth, G. A. *J. Am. Chem. Soc.* **1998**, *120*, 4006−4014.

**Table 2.** Total Energies (au), Relative Energies in Parentheses (kcal/mol), and Gas-Phase Proton Affinities PA (kcal/mol) for the **3/3$_H$** and **4/4$_H$** Mononuclear Complexes

| structures | | HF/6-31G* | ZPVE[a] | B3LYP/6-31G*//HF/6-31G* | PA[b] |
|---|---|---|---|---|---|
| $[Zn(Me\text{-}Im)_3(\mathbf{OH})]^+$ | **3** | −2644.491501 (0.0) | 0.340996 (0.0) | −2651.489602 (0.0) | − |
| $[Zn(Me\text{-}Im)_3(\mathbf{H_2O})]^{2+}$ | **3$_H$** | −2644.804825 (−196.6) | 0.353915 (8.1) | −2651.795344 (−191.8) | **184.7** |
| $[Zn(Me\text{-}Im)(SCH_3)(CH_3COO)(\mathbf{OH})]^{-1}(H_2O)$ | **4** | −2857.326865 (0.0) | 0.244665 (0.0) | −2863.645424 (0.0) | − |
| $[Zn(Me\text{-}Im)(SCH_3)(CH_3COO)(\mathbf{H_2O})](H_2O)$ | **4$_H$** | −2857.887696 (−351.9) | 0.259422 (9.3) | −2864.203989 (−350.5) | **342.6** |

[a] From HF/6-31G* analytical frequencies. [b] Using the B3LYP/6-31G* electronic energies and the HF/6-31G* thermal corrections.

**Table 3.** Total Energies (au), Relative Energies in Parentheses (kcal/mol), and Gas-Phase Proton Affinities PA (kcal/mol) of the Binuclear Zn-β-Lactamase Models Considered in This Work

| structures | | HF/3-21G* | ZPVE[a] | HF/6-31G* | B3LYP/6-31G*//HF/6-31G* | PA[b] |
|---|---|---|---|---|---|---|
| $[Zn(Me\text{-}Im)_3(\mathbf{OH})Zn(Me\text{-}Im)(SCH_3)(CH_3COO)]^+(H_2O)$ | **5** | −5399.857912 (0.0) | 0.580217 (0.0) | −5426.397541 (0.0) | −5439.313034 (0.0) | − |
| $[Zn(Me\text{-}Im)_3(\mathbf{H_2O})Zn(Me\text{-}Im)(SCH_3)(CH_3COO)]^{2+}(H_2O)$ | **5A$_H$** | −5400.197534 (−213.1) | 0.592227 (7.5) | −5426.735351 (−212.0) | −5439.649773 (−211.3) | **205.0** |
| $[Zn(Me\text{-}Im)_3(\mathbf{H_2O})Zn(Me\text{-}Im)(SCH_3)(CH_3COO)(H_2O)]2+$ | **5B$_H$** | structure not a minimum on the HF/3-21G* PES | | −5426.731500 (−209.6) | −5439.639224 (−204.7) | |
| $[Zn(Me\text{-}Im)_3(\mathbf{H_2O})Zn(Me\text{-}Im)(SCH_3)(CH_3COO)(H_2O)]2+$ | **5C$_H$** | structure not a minimum on the HF/3-21G* PES | | −5426.725407 (−205.7) | −5439.632046 (−200.2) | − |
| $[Zn(Me\text{-}Im)_3(\mathbf{OH})]^+\cdots[(CH_3COO)Zn(Me\text{-}Im)(SCH_3)\ (H_2O)]$ | **6** | −5399.872108 (0.0) | 0.579763 (0.0) | −5426.394550 (0.0) | −5439.314703 (0.0) | − |
| $[Zn(Me\text{-}Im)_3(\mathbf{H_2O})]^{2+}\cdots[(CH_3COO)Zn(Me\text{-}Im)(SCH_3)\ (H_2O)]$ | **6$_H$** | −5400.209856 (−211.9) | 0.591280 (7.2) | −5426.731500 (−211.4) | −5439.652499 (−213.0) | **206.7** |

[a] From HF/3-21G* analytical frequencies. [b] Using the B3LYP/6-31G*//HF/6-31G* electronic energies and the HF/3-21G* thermal corrections.

and they have a HF/6-31G* EPS charge of 1.01 e (1.40 e in **1$_H$**). The corresponding Zn−N BCP properties more clearly reflect the effects of ligand substitution. The imidazole ring increases the Zn−N $\rho(\mathbf{r_c})$ values by 15%, and the local energy density increases by ∼20% which is indicative of the increased donor ability of the imidazole ligands.

The mononuclear complexes **4$_H$/4** in Figure 2 model the two different protonation states of the Zn2 binding site in the binuclear β-lactamases as liganded by the corresponding amino acid side chains. In both complexes the Zn ion is 4-coordinated, and the second water molecule is most favorably located in an intermediate position between the Zn-bound water/hydroxide moieties and the imidazole ring (see Figure 2). Comparing the HF/6-31G* data for **4$_H$/4** with those for **2$_H$/2**, we see that replacement of ammonia by imidazole, formate by acetate, and sulfide by methylthiolate results in slight changes in the Zn−ligand bond distances and BCP properties. Moreover, the EPS charges on the Zn ion are similar and a more basic Zn-bound hydroxide. The calculated PA increases about 10 kcal/mol (see Table 2). In general these changes are less important than those observed on going from **1$_H$/1** to **3$_H$/3**, reflecting that the Zn2 ion is effectively placed in a harder cavity with respect to the Zn1 binding site.

Examination of the mono-zinc complexes **3$_H$/3** and **4$_H$/4** gives some insight into the coordination ability of the Zn1 and Zn2 ions in the *B. cereus* and *B. fragilis* enzymes. Nevertheless, geometry optimizations of binuclear model compounds and the subsequent analysis and comparison with experimental data are indispensable to obtain further insights into the structure, protonation state, and mechanism of the Zn β-lactamases.

**Binuclear Complexes.** By taking into account our previous computational experience on zinc metallo-enzymes[45,46] and the relatively large size of the *B. fragilis* active site, the capability of the standard PM3 Hamiltonian to describe Zn binuclear complexes was first investigated. Unfortunately, we found that the fully optimized PM3 geometries for the corresponding conjugate acid−base pair differ substantially from the experimental *B. fragilis* structure in either the coordination around the Zn ions or the number and type of Zn−ligand contacts (PM3 data not shown for brevity).

Figures 3−8 give the HF/6-31G* optimized geometries and critical EPS charges for the series of binuclear complexes studied in this work, while Table 3 contains the corresponding total and relative energies. The first series of compounds we looked at is composed of one basic structure (**5** in Figure 3) and three different protonated isomers (**5A$_H$**, **5B$_H$**, and **5C$_H$** in Figures 4−6, respectively). Interestingly, the Zn1 and Zn2 ions are bridged by a hydroxide moiety in this family of structures in agreement with available experimental evidence. On the other hand, the acid−base pair **6/6$_H$** in Figures 7−8 is best described as supramolecular arrangements of two mononuclear Zn complexes in which the two Zn ions do not have a common ligand.

The overall charge (+1) and protonation state of the basic form **5**, $[(Me\text{-}Im)_3Zn-(OH)-Zn(CH_3S)(CH_3CO_2)(Me\text{-}Im)]^+(H_2O)$, is comparable to those of the active site assumed in the recently proposed mechanism for the mode of action of the *B. fragilis* enzyme.[22] In general, with respect to the mono-zinc structures **3** and **4**, the coordination environments of the Zn1 and Zn2 ions in **5** show moderate structural and electronic changes (see Figures 2−3). The HF/6-31G* Zn1···Zn2 distance (3.544 Å) is quite close to the experimental value of ∼3.5 Å.[14] The shared hydroxide shows a typical H-bond contact with the carboxylate O atom in the Asp group (the HF/6-31G* O−H···O distance and $\rho(\mathbf{r_c})$ value are 1.956 Å and 0.027 au,

(45) (a) Toba, S.; Colombo, G.; Merz, K. M., Jr. *J. Am. Chem. Soc.* **1999**, *121*, 2290−2303. (b) Merz, K. M., Jr.; Banci, L.; *J. Am. Chem. Soc.* **1997**, *119*, 863−871.

(46) (a) Merz, K. M., Jr.; Banci, L. *J. Phys. Chem.* **1996**, *100*, 17414−17420. (b) Hartsough, D. S.; Merz, K. M., Jr. *J. Phys. Chem.* **1995**, *99*, 11266−11275.

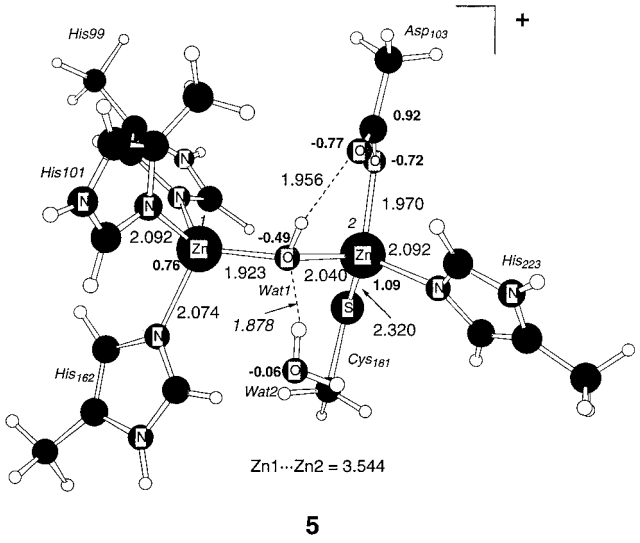


**Figure 3.** Optimized structure of the binuclear complex **5**. HF/6-31G* distances in Å. The most relevant ESP charges with attached hydrogens summed into the heavy atoms are also indicated in boldface characters.

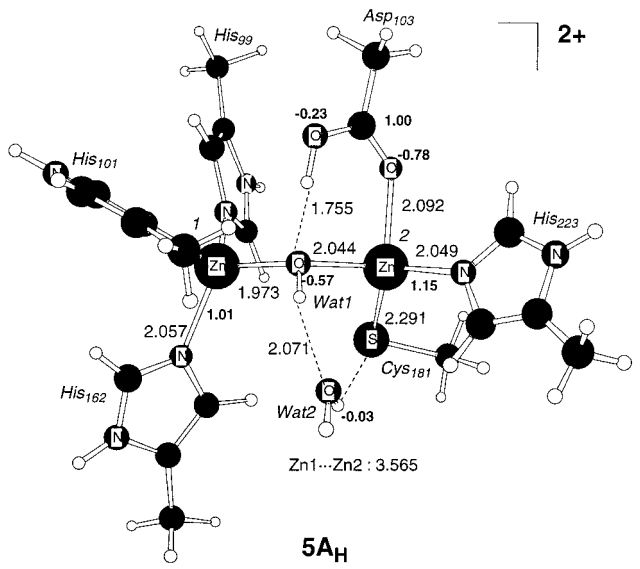


**Figure 4.** Optimized structure of the binuclear complex $\mathbf{5A_H}$. HF/6-31G* distances in Å. The most relevant ESP charges with attached hydrogens summed into the heavy atoms are also indicated in boldface characters.

respectively). However, as in the case of the mononuclear complexes **2** and **4**, the Zn2 site in **5** presents a distorted tetrahedral coordination, while the Wat2 molecule forms a short H bond with the Zn-bound Wat1. This is in contrast with the *B. fragilis* X-ray structure in which the Wat2 molecule is directly coordinated to the Zn2 position. Despite an intensive search on the HF/6-31G* PES, we could not locate other binuclear isomers related to the basic form **5**.

The binuclear model $\mathbf{5A_H}$, which represents a monoprotonated active site with a global charge of +2, can be considered as the conjugate acid of **5** (see Figures 3 and 4). The equilibrium Zn1···Zn2 distance in $\mathbf{5A_H}$ is 3.565 Å, only 0.021 Å longer than that found in **5**. The rest of Zn−ligand bonds including the Zn1−Wat1 and Zn2−Wat2 bonds show only moderate differences with respect to **5**. Thus, an increase of the global charge of the model only slightly influences the $Zn^{2+}\cdots Zn^{2+}$ repulsion or the basic structural elements of the Zn binuclear complexes. The most significant change concerns the O−H···O contact between

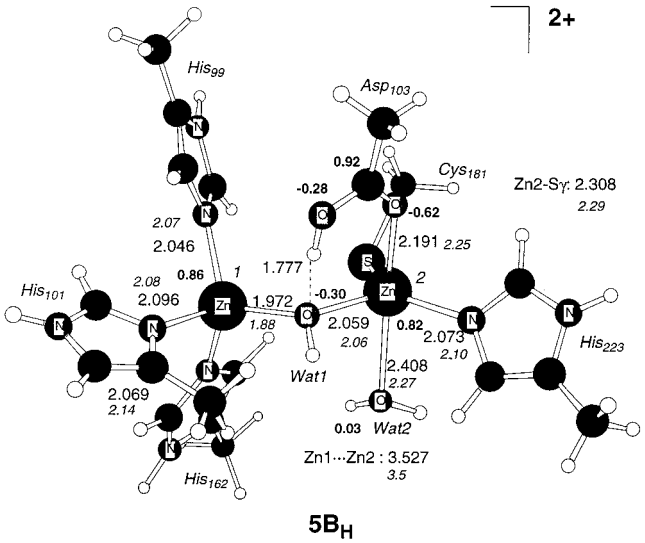


**Figure 5.** Optimized structure of the binuclear complex $\mathbf{5B_H}$. HF/6-31G* distances in Å. Figures in italic characters correspond to X-ray distances. The most relevant ESP charges with attached hydrogens summed into the heavy atoms are also indicated in boldface characters.

the Asp group and Wat1. In fact, the shared water molecule directly transfers one proton to the carboxylate group to give an hydroxide group which bridges the two zinc ions. Simultaneously, the hydroxide ion forms an H bond with the carboxylic acid moiety of the resultant neutral Asp residue (the HF/6-31G* O−H···O distance and $\rho(\mathbf{r_c})$ values are 1.755 Å and 0.040 au, respectively). The calculated PA of the $\mathbf{5A_H/5}$ pair is 206.0 kcal/mol, 20.3 kcal/mol higher than that of $\mathbf{3_H/3}$.

The monoprotonated isomer $\mathbf{5B_H}$ in Figure 5, which is 2.4 and 6.6 and kcal/mol less stable than $\mathbf{5A_H}$ at the HF/6-31G* and B3LYP/6-31G*//HF/6-31G* levels, reproduces the essential characteristics of the *B. fragilis* active site, the Zn1 and Zn2 ions having tetrahedral and trigonal bipyramidal environments, respectively. The Wat2 molecule in $\mathbf{5B_H}$, which hydrates the bridging hydroxide moiety in $\mathbf{5A_H}$, is bound directly to the Zn2 position (bond distance of 2.408 Å). Inspecting the Zn−Wat2 BCP properties ($\rho(\mathbf{r_c}) = 0.028$ and $H(\mathbf{r_c}) = +0.0003$ in au), confirms that this bond is much weaker than the rest of the Zn−ligand bonds in $\mathbf{5B_H}$, and therefore, Wat2 likely could be readily displaced. The rest of geometrical features of $\mathbf{5A_H}$ and $\mathbf{5B_H}$ are quite similar. As in $\mathbf{5A_H}$, the neutral Asp ligand would interact with the zinc-bridging hydroxide moiety via a strong O−H···O interaction with a distance of 1.777 Å and a $\rho(\mathbf{r_c})$ value of 0.038 au. It may be worth noting that $\mathbf{5B_H}$ does not correspond to a stable minimum on the HF/3-21G* PES. The inclusion of electron correlation in the calculation should stabilize the $\mathbf{5B_H}$ structure by reinforcing the Zn2−Wat2 and the OH(Asp)···O(Wat1) interactions (see above).

For comparative purposes, Figure 5 also includes some X-ray bond distances that show a reasonable agreement with the theoretical values computed for the complex $\mathbf{5B_H}$ and with those for $\mathbf{5A_H}$ and **5** as well. To further discriminate between these theoretical structures, the O(Wat1)···O$\delta$2(Asp) distance and the O(Wat1)−O$\delta$2(Asp)−C$\gamma$(Asp)−O$\delta$1(Asp) torsion angle was used. The O(Wat1)···O$\delta$2(Asp) distance has values of 2.81, 2.69, 2.73, and 2.68 Å in **5**, $\mathbf{5A_H}$, $\mathbf{5B_H}$, and the X-ray[14] structure, respectively, while the corresponding torsion angle values are 23.8, 3.0, −4.8 and 11.4°. Thus, the hydroxide moiety present in the X-ray structure and in models $\mathbf{5A_H}$ and $\mathbf{5B_H}$ is more coplanar with the Asp carboxylate group than in the basic model **5**. Overall the monoprotonated model system $\mathbf{5B_H}$ compares

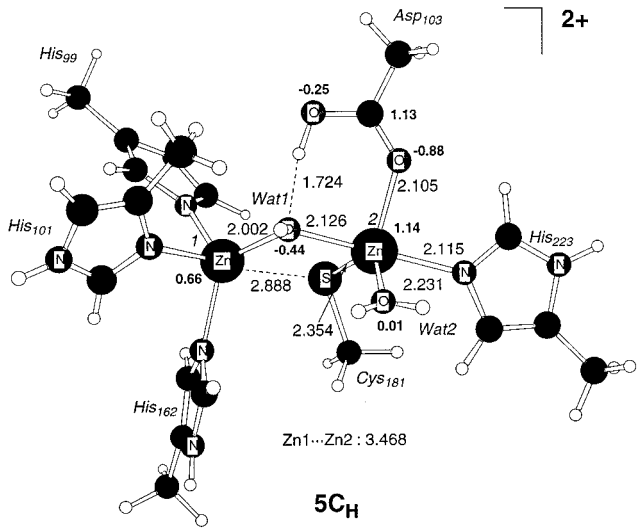


**Figure 6.** Optimized structure of the binuclear complex $\mathbf{5C_H}$. HF/6-31G* distances in Å. The most relevant ESP charges with attached hydrogens summed into the heavy atoms are also indicated in boldface characters.

favorably with respect to the experimentally observed structure of the *B. fragilis* active site.

The third protonated form located on the HF/6-31G* PES corresponds to the complex $\mathbf{5C_H}$ in Figure 6. At the HF/6-31G* and B3LYP/6-31G*//HF/6-31G* levels, $\mathbf{5C_H}$ is 6.3 and 11.1 kcal/mol less stable than $\mathbf{5A_H}$, respectively. Examination of the $\mathbf{5C_H}$ structure shows that this model reproduces some structural features of the *B. fragilis* active site: the Zn1···Zn2 distance is 3.468 Å, while the Zn2−Wat2 distance (2.231 Å) and the Zn−O(Wat2) $\rho(\mathbf{r_c})$ value (0.039 au) confirm that Wat2 is directly coordinated to the Zn2 ion. However, $\mathbf{5C_H}$ differs sharply from the crystallographic structure given that the methylthiolate ligand bridges the two Zn ions in $\mathbf{5C_H}$. The corresponding Zn1−S and Zn2−S distances are 2.888 and 2.354 Å, whereas the X-ray values are 4.2 and 2.3 Å.[14] The location of one HF/6-31G* BCP with a $\rho(\mathbf{r_c})$ value of 0.007 au, further characterizes the Zn1···methylthiolate interaction. This structural discrepancy with experiment and its relative instability with respect to $\mathbf{5A_H}$ and $\mathbf{5B_H}$ discards $\mathbf{5C_H}$ as a β-lactamase model for the ground state of the *B. fragilis* active site.

As discussed above, the second set of binuclear structures $\mathbf{6/6_H}$ (see Figures 7 and 8) lack the hydroxide-mediated Zn1···Zn2 interaction. The absence of this interaction has been reported in the X-ray structure[8] of the binuclear β-lactamase from *B. cereus*, and therefore, the $\mathbf{6/6_H}$ complexes might be considered as models for zinc binding to the *B. cereus* active site. Both Zn ions in $\mathbf{6/6_H}$ have 4-coordination, but the Zn1···Zn2 distances are 4.485 and 5.931 Å in the basic form **6** and the conjugate acid $\mathbf{6_H}$, respectively. The basic structure **6** has the hydroxide moiety directly bound to the Zn2 position (Zn2−OH: 1.948 Å). Both the Zn2-bound hydroxide and the Asp in **6** act as donors in two H bonds with the Zn1-bound water molecule, which results in the much shorter Zn···Zn distance. For the acid isomer $\mathbf{6_H}$, the Zn1-bound water retains both H atoms and establishes one strong H bond with the negatively charged Zn2 Asp group. Despite their considerable geometrical differences, the $\mathbf{6_H/6}$ and $\mathbf{5A_H/5}$ pairs have similar calculated PA (206.0 and 205.0 kcal/mol, respectively). Most interestingly, the loss of the hydroxide-mediated Zn1···Zn2 bond through either the $\mathbf{5 \rightarrow 6}$ or $\mathbf{5A_H \rightarrow 6_H}$ rearrangements is slightly exoergic by 1.0 and 1.7 kcal/mol, respectively, at the B3LYP/6-31G*//HF/6-31G* level. These small energy differences could have mechanistic consequences for the catalytic action of the *B. fragilis* enzyme.

## Discussion

By comparison with the crystallographic coordinates, the HF/6-31G* structural data presented above suggests that the actual protonation state of the *B. fragilis* active site would have a global charge of +2 and a Zn1−OH···HOOC(Asp)−Zn2 interaction similar to that observed in the β-lactamase model $\mathbf{5B_H}$. The presence of two buried aspartate residues[14] ($Asp_{69}$, $Asp_{165}$) associated with the *B. fragilis* active site could provide a favorable environment for the accumulation of positive charge in the active site. However, based solely on the structural analysis, our predictions about the charge distribution in the *B. fragilis* active site are not firmly established. Therefore, other energetic, electronic, and mechanistic aspects need to be discussed further to support complex $\mathbf{5B_H}$ as the best theoretical model for the *B. fragilis* active site observed in the X-ray structure.

**Charge Distribution and Zinc Affinity.** As discussed above one of the most interesting characteristics of β-lactamase from *B. fragilis* is that the enzyme strongly binds two zinc ions with comparable affinity.[14] According to our analyses on the Zn1 ($\mathbf{3_H/3}$) and Zn2 ($\mathbf{4_H/4}$) mononuclear complexes, the corresponding acid isomers $\mathbf{3_H}$ and $\mathbf{4_H}$ bind the $Zn^{2+}$ ions within a *soft* cavity, which minimizes the positive charge on the Zn ions and strengthens the Zn−ligand interactions relative to the basic forms **3** and **4**. Apart from the presence of the weak Zn2−Wat2 interaction in $\mathbf{5B_H}$, the binuclear complexes do not dramatically differ from their respective mononuclear counterparts. Interestingly, we see in Figures 3 and 5 that the Zn1 and Zn2 ions in $\mathbf{5B_H}$ have similar charges of +0.86 and +0.82 e, respectively, whereas the corresponding charges in the basic form **5** are markedly different, +0.76 and +1.09 e, respectively. Therefore, both the geometry and the charge distribution of the binuclear model $\mathbf{5B_H}$ support the existence of two zinc binding sites with equal zinc affinity, while the Zn1 and Zn2 sites in the basic structure **5** would most likely present a dissimilar zinc affinity.

**p$K_a$ of Catalytically Important Groups.** Steady-state and transient-state kinetic studies of the *B. fragilis* catalytic process have not found a pH dependence through a pH range of 5.25 to 10.0.[20] It therefore appears that there are no ionizable groups with p$K_a$ values in the interval 5.25−10.0 involved in catalysis. It is well known that the p$K_a$ of a Zn-bound water in carbonic anhydrases is around 7, the deprotonated form being the most favorable one at neutral pH. Thus, it has been assumed that the p$K_a$ value of the *B. fragilis* nucleophilic center, normally postulated to exist in the form of the hydroxide molecule (Wat1), would have a low p$K_a$ value due to the effects of the two zinc ions.

Our calculations predict that the $\mathbf{5A_H/5}$ pair has a PA which is 20 kcal/mol higher than that of the Zn-bound water in $\mathbf{3_H/3}$ which mimics the carbonic anhydrase active site. Interestingly, the Zn2−Wat1 bond is altered as a consequence of the protonation ($\mathbf{5 \rightarrow 5A_H}$) process. Therefore, with respect to the $\mathbf{3_H/3}$ acid−base pair, the greater PA of $\mathbf{5A_H/5}$ may stem from the preferential stabilization of $\mathbf{5A_H}$ due to the much stronger Zn1−O−H···HOOC(Asp)−Zn2 interaction than the Zn1−O−H···$^-$OOC(Asp)−Zn2 in the basic form **5**. To further support this interpretation, we calculated the binding energy between an acetate ion and a water molecule. At the B3LYP/6-31G* level including the ZPVE correction, the $CH_3COO^-\cdots H_2O$ binding energy amounts to 18.8 kcal/mol (17.4 kcal/mol using CCSD(T) and MP2 composite electronic energies). These values

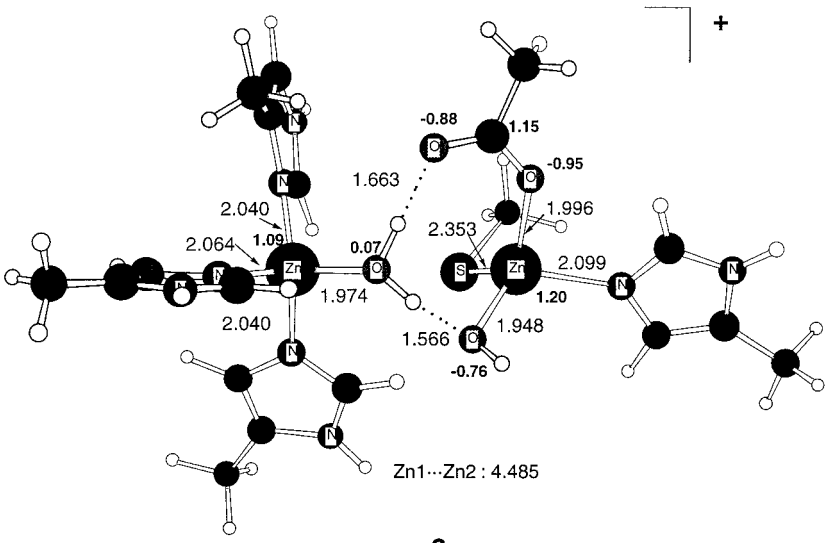


**Figure 7.** Optimized structure of the binuclear complex **6**. HF/6-31G* distances in Å. The most relevant ESP charges with attached hydrogens summed into the heavy atoms are also indicated in boldface characters.

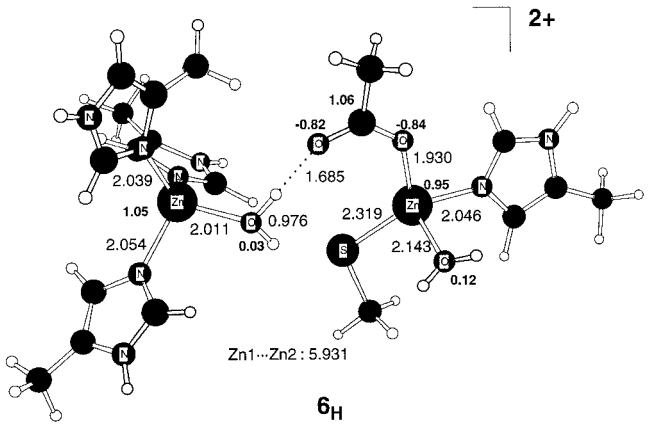


**Figure 8.** Optimized structures of the binuclear complex $\mathbf{6_H}$. HF/6-31G* distances in Å. The most relevant ESP charges with attached hydrogens summed into the heavy atoms are also indicated in boldface characters.

are similar to the PA difference between the $\mathbf{3_H/3}$ and $\mathbf{5A_H/5}$ pairs (20.3 kcal/mol at the B3LYP/6-31G*//HF/6-31G* level).

Although the protein matrix of zinc enzymes will play a role in determining the actual p$K_a$ of the Zn-bound groups,[40b] it is the zinc ion and its ligand environment that play a primary role. Hence, we expect that our in vacuo binuclear models partially account for most of the pH dependence observed experimentally.[20] When the Zn1−O−H···HOOC(Asp)−Zn2 interaction is present in the monoprotonated models $\mathbf{5A_H}$ and $\mathbf{5B_H}$, the zinc-bound Wat1 molecule closely resembles an hydroxide moiety (basic site), while the Zn2-bound Asp group constitutes the protonated end of the O−H···O contact (acid site). Since this H-bonding interaction locks up the acidic proton in a strong H-bonding interaction a high p$K_a$ might be possible. Moreover, since the $\mathbf{5A_H/5}$ pair has a relatively high PA, a p$K_a$ value of >10.0, formally assigned to the Asp group which is protonated in the $\mathbf{5A_H}$ and $\mathbf{5B_H}$ structures, would be possible. On the other hand, the low p$K_a$ group in the *B. fragilis* active site, in this scenario, would correspond to the basic site, that is, the Zn1-bound Wat molecule, which is unprotonated at the biologically relevant pH range. The presence of the strong OH···O contact can explain the stability and the absence of a pH dependence in catalysis by *B. fragilis* enzyme for the pH range 5.25−10.0.

**Scheme 5**

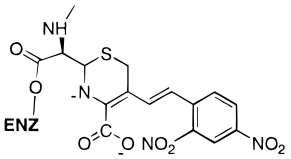


This proposed protonation state for the *B. fragilis* active site is in agreement with that postulated for many mononuclear zinc hydrolases which show a (Glu)$COO^-$−$OH_2$−Zn linkage whose monoprotonated form corresponds to the active structure.[24]

Full protonation of the active site would result in the rupture of the Zn1−O−H···HOOC−Asp-Zn2 interaction, thereby, removing the nucleophilic ability of the resultant binuclear zinc structure. This observation would explain the experimentally observed loss of enzyme activity at low pH.[20] Conversely, at high pH, the basic form **5** would represent the predominant protonation state for the *B. fragilis* active site.

**Substrate and Intermediate Binding to *β*-Lactamase Models.** Several models for substrate binding to the binuclear Zn active site of metallo-*β*-lactamases have been generated on the basis of the three-dimensional structures.[14,15] In all of the models, the enzymes can accommodate a variety of *β*-lactam antibiotics, the Zn sites being favorably located to polarize the *β*-lactam amide group: Zn1 interacts with the carbonyl group of the *β*-lactam ring, while Zn2 is in close proximity to the *β*-lactam N atom. The docking analyses also indicate that the Zn2-bound Wat2 molecule could be displaced when substrate is bound.

Recent experimental studies[21,22] on nitrocefin degradation have observed that the *B. fragilis* mechanism has a rate-determining step that involves the breakdown of the intermediate in which the endocyclic N in the nitrocefin *β*-lactam is unprotonated (see Scheme 5). It has been proposed that this doubly charged intermediate would be stabilized by electronic conjugation between the negative charge on the N atom and the 2,4-dinitrostyryl substituent as well as through strong electrostatic interactions between the acyl intermediate and Zn2 in the active site. Indeed, substrate-binding should be more favorable for the doubly charged *β*-lactamase models, $\mathbf{5A_H}$ and $\mathbf{5B_H}$, than for the basic one, **5**, with a lower global charge of +1.

**Scheme 6**

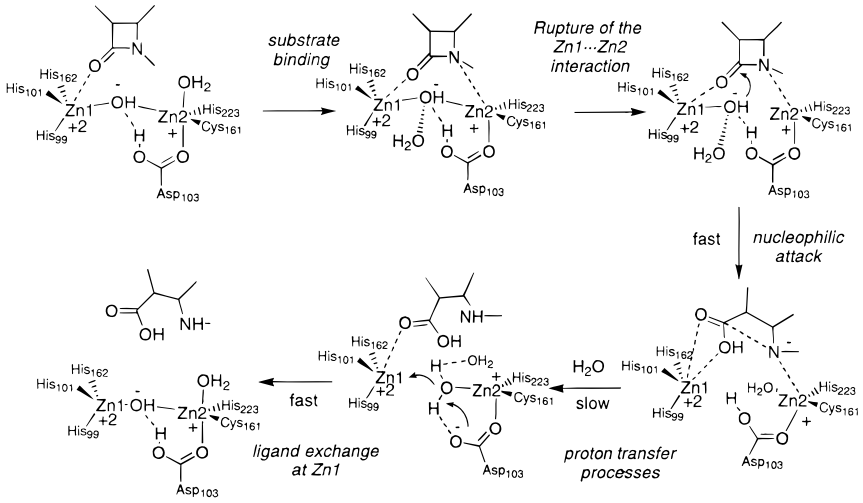


Another aspect supporting the assignment of the monoprotonated form of the *B. fragilis* active site as the most versatile one is through the characterization of various isomeric forms of the binuclear active site which are close in energy but show significant changes in the coordination sphere around the Zn2 ion. Clearly, the protein environment and substrate-binding would influence the relative stability of the series of structures **5A$_H$**, **5B$_H$**, **5C$_H$**, and **6$_H$**. However, the observed flexibility of the Zn2-bound ligands, especially that of the Wat1 and Wat2 ligands, may play a significant role in the catalytic mechanism (see below).

**Comparison of the *B. cereus* and *B. fragilis* Active Sites.** In contrast with the *B. fragilis* enzyme, the reported structures[6,8,9] for the *B. cereus* enzyme containing two zinc ions show Zn2 environments which are not readily comparable with the HF/6-31G* models **6$_H$/6**. For example, the Zn2 site in the experimental X-ray structure, discussed by Fabiane et al.,[8] has a very "loose" and flexible arrangement of ligands in which the X-ray Zn2···Wat2 and Zn2···O$\delta$(Asp) distances have values of 2.5−3.1 Å and 2.8−2.9 Å, respectively, while the Zn1···Zn2 contacts are 3.9 and 4.4 Å for the two protein molecules present in the unit cell. The experimental Zn2−S$\gamma$(Cys) distance (∼2.0 Å) is even shorter than that found in a monodentate $[Zn(SCH_3)]^+$ complex at the HF/6-31G* (2.168 Å) and B3LYP/6-31G* (2.142) levels of theory.

Clearly, the structure of the binuclear active site in the *B. cereus* enzyme is more strongly affected by the protein environment, and these effects have not been fully considered in our **6$_H$/6** model systems. Nevertheless, some insight into the differences in the structures of the *B. cereus* and *B. fragilis* enzymes could be derived from our calculations. Particularly, the different affinity of the *B. cereus* enzyme for the two Zn sites could be rationalized in terms of a different protonation state with respect to that in the *B. fragilis* enzyme. The basic form with a global charge of +1 (i.e., Wat1 present as a hydroxide nucleophile and the negatively charged Asp and Cys groups coordinating the Zn2 ion) would be most compatible with the low Zn2 affinity exhibited by the *B. cereus* enzyme. Another structural characteristic of the *B. cereus* enzyme[8,9] results from the presence of a positive charge (Arg/Lys groups) at distance of around 4 Å from the Zn2 site which may decrease the Zn2-binding constant. Conversely, for the *B. fragilis* enzyme, the closest positively charged group to the active-site corresponds to a $Na^+$ ion which is 6 Å away from Zn2 and should not interfere with Zn2 binding.[14]

The change in the protonation state between the *B. fragilis* and *B. cereus* enzymes is not only consistent with their markedly different structure but also with the different pH dependence of their catalytic behavior and the mechanistic role played by the Zn2 ion. The decrease of the $k_{cat}/K_m$ for the *B. cereus* enzyme with the second power in $[H^+]$ below pH 5 has been interpreted in terms of the simultaneous presence of Wat1 and the Asp residue in their deprotonated forms.[10] However, as previously mentioned for the *B. fragilis* enzyme, the fact that Wat1 and the Asp group establish a short O−H···O interaction is consistent with the absence of an experimentally observed pH dependence. Moreover, since the ligand binding ability of the Zn2 ion in the *B. cereus* active site is low, this Zn2 ion could only play a minor mechanistic role in the hydrolysis of β-lactam substrates in agreement with all of the experimental evidence.[6−10]

## Conclusions

**Mechanistic Implications for the *B. fragilis* Mode of Action.** By combining the results from the substrate-binding analyses and the structural and energetic data on the β-lactamase model compounds, several chemical events, which are likely to occur during the catalytic hydrolysis of β-lactams by *B. fragilis*, can be assessed.

Expanding on the mechanistic proposals of Wang et al.,[22] we sketch in Scheme 6 a possible mode of action of the *B. fragilis* enzyme in which the binuclear Zn active site has a global charge of +2 instead of the initially assumed charge of +1. We note that the β-lactamase models **5A$_H$** and **5B$_H$** do maintain the catalytic advantage in having the Zn-bridging hydroxide moiety as the deprotonated nucleophile, while their excess of global charge would facilitate the activation of the negatively charged substrate and the formation of the key intermediate. In the ground-state structure of the enzyme, the Zn2-bound Asp carboxylate group can be formally considered to accept a proton from the Wat1 molecule, thereby acting as an internal base that "promotes" the nucleophilicity of Wat1. Both the zinc hydroxide and the Asp residue are the main functional groups conserved in the different zinc-β-lactamases, as well as in zinc peptidases.[24]

For the model **5B$_H$**, which would represent the native structure of the active site, the Zn2-bound Wat2 molecule can be readily displaced to facilitate β-lactam binding (see above). In fact, the **5A$_H$** isomer shown in Figure 4 could be stabilized by means of substrate binding through the vacant coordination position at Zn2. As in ref 22, we postulate that the rupture of the hydroxide-

mediated Zn1···Zn2 interaction is induced upon substrate binding, thereby releasing the Wat1 hydroxide nucleophile to attack the $\beta$-lactam carbonyl group without serious steric constraints. This rearrangement should not be an unfavorable process because of the moderate energy differences along the series of structures $\mathbf{5A_H}$, $\mathbf{5C_H}$, and $\mathbf{6_H}$. A binuclear structure like $\mathbf{5C_H}$, in which the Zn2−Wat1 is weakened with respect to $\mathbf{5A_H}$, may be involved in the rupture of the Zn2−Wat1 bond if Wat2 was replaced by the substrate.

After cleavage of the Zn2 hydroxide bond, the Zn1 and Zn2 ligand environments would be linked by the Asp-Wat1 contact and, most likely, by the $\beta$-lactam amide functionality as well. In this hypothetical complex precursor of the acyl enzyme intermediate, the nucleophilic attack on the $\beta$-lactam carbonyl should be very favorable both geometrically and electronically, though this still needs to be verified computationally. Nonetheless, as in the case of the mono-zinc enzymes, the Zn1··· carbonyl interaction can polarize the C−O bond and place the hydroxide nucleophile in such a way that it can readily attack the carbonyl carbon. With respect to the alkaline hydrolysis of $\beta$-lactams in aqueous solution,[1] the main catalytic role of Zn1 would consist of providing a desolvated and properly oriented *hard* nucleophile in the form of the Zn-bound hydroxide moiety, thereby reducing the barrier height for the nucleophilic attack relative to an aqueous environment.[27] The neutral Asp group linked to the nucleophile by the O−H···O contact would play a passive role, stabilizing the configurations along the reaction pathway.

Computational studies on model systems have shown that the formation of the C−O bond in alkaline hydrolysis strongly affects the C−N endocyclic bond of $\beta$-lactams by developing a partial negative charge on the N atom. This facilitates the formation of very labile intermediates, which have varying degrees of C−N cleavage.[26−28] In the case of the *B. fragilis* active site, both experimental and theoretical results indicate that the accumulation of charge on the N atom can be stabilized either by conjugation or by nitrogen coordination to the Zn2 site. In fact, the formation of the dianionic intermediate, characterized by a strong Zn2···N($\beta$-lactam) interaction, should increase the stability of the Zn2 coordination environment which was partially lost in the initial stages of the process. Consequently, the average life of the anionic acyl enzyme species would be much greater than that of the nonenzymatic process.

The release of the intermediate requires that the $\beta$-lactam N atom becomes protonated.[27] According to kinetic data, the proton rearrangement constitutes the rate-determining step of the process. Besides favoring substrate activation and intermediate formation, the presence of the second zinc will influence the mechanism of the proton-transfer steps necessary to complete the hydrolysis process. Several sequences of proton transfers involving the hydroxyl group of the acyl enzyme or a water molecule weakly coordinated to Zn2 may account for this process. We predict that the Zn2-bound Asp group could also participate as a proton shuttle or proton donor in a way similar to that of the proposed situation for the *B. cereus* enzyme.[10] Although the exact details of the proton-transfer events remain unknown, the origin of the energy barrier can arise from the destabilization of the Zn2 environment and the loss of conjugation of the negative charge at the initial stages of proton transfer. Scheme 6 depicts a possible structure for a product−enzyme complex. For this intermediate structure, we assume that the Zn2 site would adopt 4-coordinate structure (similar to that of $\mathbf{4_H}$ in Figure 2) through the formation of a Zn2−Wat bond. The Wat2 ligand in the native structure of the enzyme is a reasonable candidate for replacing the Zn-substrate coordination at the end of the hydrolysis process. Finally, through deprotonation via the Asp group, the hydroxide can be regenerated, thereby completing the ligand exchange at the Zn1 site and final formation of the binuclear structure of the active site ready for the next turnover (see Scheme 6).

**Differences and Similarities in the Mode of Action of Metallo-*β*-Lactamases.** The zinc-$\beta$-lactamases have substantial differences in their structure and mechanism of action. For the *B. fragilis* and *B. cereus* active sites, the Zn2 binding site has specific coordination abilities and functions in each enzyme. However, in both enzymes as well as in other $\beta$-lactamases (e.g., the binuclear enzyme from *Stenotrophomonas maltophila*[11,12]) the more general mechanistic pattern of dinuclear hydrolases can be elucidated. One of the zinc ions, tightly bound to the enzyme, provides a metal-bound hydroxide moiety properly placed for nucleophilic attack while the other zinc ion mainly influences the nature of the anionic intermediate and the mechanism of the rate-determining proton transfer to the $\beta$-lactam N atom. However, the first zinc ion (Zn1) is the essential one for the catalytic activity of all the zinc $\beta$-lactamases, whereas the lack or presence of the Zn2 ion would control the enzyme efficiency by modifying the mechanism of N protonation. Our calculations have shown that the Zn2 environment, which includes a mixture of *hard*−*soft* and charged−neutral ligands, exhibits a flexible and complex coordination ability that can take advantage of evolutionary changes. On the other hand, the Zn1 environment is much less altered along the series of mononuclear and binuclear models studied herein. Therefore, it could be postulated that the critical nucleophilic addition of the Zn1 hydroxide to the $\beta$-lactam carbonyl group would take place through a transition structure fairly invariant among the different zinc-$\beta$-lactamases. These results suggest that the design of compounds capable of mimicking the transition state[47] for the zinc hydroxide nucleophilic attack to $\beta$-lactams, could eventually lead to the synthesis and application of generic zinc-$\beta$-lactamases inhibitors.

**Acknowledgment.** We thank the NIH for supporting this research through Grant GM44974. We also thank the Pittsburgh Supercomputer Center, National Center for Supercomputer Applications, San Diego Supercomputer Center, and the Cornell Theory Center for generous allocations of supercomputer time. N.D. and D.S. thank DGSIC (MEC-Spain) for partial support of this work via Grants PB-98-44430549 and EX-99-10863995Z, respectively.

**Supporting Information Available:** Table of BCP properties for all of the structures in Figures 1−8, molecular geometries of the $\mathbf{3_H/3}$ and $\mathbf{4_H/4}$ mononuclear species and all of the binuclear complexes (PDF). This material is available free of charge via the Internet at http://pubs.acs.org.

JA994462S

(47) Vahrenkamp, H. *Acc. Chem. Res.* **1999**, *32*, 589−596.